

Polarization Switching Dynamics Governed by Thermodynamic Nucleation Process in Ultrathin Ferroelectric Films

J. Y. Jo,¹ D. J. Kim,¹ Y. S. Kim,¹ S.-B. Choe,¹ T. K. Song,² J.-G. Yoon,³ and T. W. Noh^{1,*}

¹*School of Physics and Astronomy, Seoul National University, Seoul 151-747, Korea*

²*School of Nano & Advanced Materials University,*

Changwon National University, Changwon, Gyeongnam 641-773, Korea

³*Department of Physics, University of Suwon, Suwon, Gyeonggi-do 445-743, Korea*

(Dated: June 13, 2018)

A long standing problem of domain switching process - how domains nucleate - is examined in ultrathin ferroelectric films. We demonstrate that the large depolarization fields in ultrathin films could significantly lower the nucleation energy barrier (U^*) to a level comparable to thermal energy ($k_B T$), resulting in power-law like polarization decay behaviors. The “Landauer’s paradox”: U^* is thermally insurmountable is not a critical issue in the polarization switching of ultrathin ferroelectric films. We empirically find a universal relation between the polarization decay behavior and $U^*/k_B T$.

PACS numbers: 77.22.Ej, 77.80.Fm

Recent advances in complex oxide thin film synthesis and in first-principles calculations have intensified the basic research on ferroelectricity at nanoscale dimension [1, 2]. The cooperative nature of ferroelectricity is expected to induce different polarization states at nanoscale due to low-dimensional boundary conditions and the strong interactions of polarization with strain, charge, and other electromechanical parameters [1, 2, 3, 4, 5, 6, 7]. Many workers have reported intriguing physical phenomena occurring in ultrathin ferroelectric (FE) films and other nanostructures, such as intrinsic size effects [1, 2, 3], strain-enhanced FE properties [4], unusual low-dimensional phases [5], and domain patterns [6, 7]. On the other hand, the mechanism and domain dynamics of FE switching in ultrathin films have rarely been investigated in spite of their scientific and technological importance [8, 9, 10].

Historically, the mechanism of polarization switching dynamics in ferroelectrics has been the subject of a great deal of research. It is now believed that the polarization switching takes place not by coherent switching, but by the nucleation and growth of new domains [8, 9, 10]. However, there still remains an unsolved issue: How do the domains nucleate? In the late 1950s, Landauer emphasized that a thermodynamic nucleation process cannot play a role in FE domain switching [11]. For a nucleus with reversed polarization to be created by a thermodynamic process, an energy barrier for nucleation U^* should be thermally overcome, as shown in Fig. 1(a). However, Landauer’s and later estimates showed that U^* is practically insurmountable by the thermal activation process: $U^* > 10^8 k_B T$ at an electric field $E \sim 1$ kV/cm (a typical value of the coercive field for bulk ferroelectrics) [11] and $U \sim 10^3 k_B T$ at $E \sim 100$ kV/cm (a typical value of the coercive field for most FE thin films) [10, 13], where k_B is Plank’s constant and T is temperature. According to these estimates, it is difficult to understand the observed domain nucleation in ferroelectrics. This problem

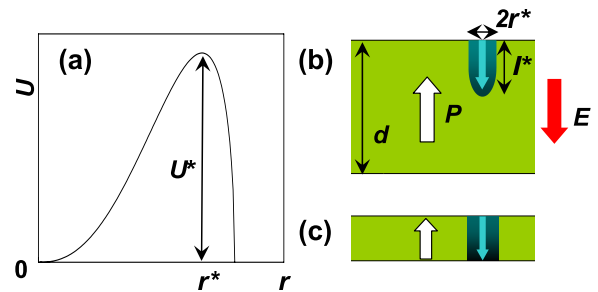


FIG. 1: (color online). (a) A schematic diagram of electrostatic energy for the nucleus formation (U) as a function of the nuclear radius (r). Schematic diagrams of (b) the half-prolate spheroidal nucleus formation and (c) the cylindrical nucleus formation, with reversed polarization.

has been known as the “Landauer’s paradox”. To overcome this difficulty, numerous workers have assumed that the nuclei could be formed inhomogeneously due to external effects, such as defects [12], long-range interaction between nuclei [13] and FE-electrode coupling [14]. However, in this Letter, we will demonstrate that U^* could be thermally overcome in the ultrathin FE film. The thermodynamic nucleation of reversed domains due to a large depolarization field E_d can govern the polarization switching process, without inclusion of any external effects, in ultrathin epitaxial BaTiO_3 films.

Fully strained $\text{SrRuO}_3/\text{BaTiO}_3/\text{SrRuO}_3$ capacitors of high quality were fabricated using pulsed laser deposition with reflection high-energy electron diffraction [1]. The thickness of BaTiO_3 (d_{BTO}) is between 5.0 and 30 nm. We were able to directly measure P - E hysteresis loops and polarization decay behaviors even for a 5.0 nm thick BaTiO_3 film [1, 15, 16]. We focused on the polarization decay behaviors for different BaTiO_3 film thickness and measurement conditions. As shown in Fig. 2(a), these $\text{SrRuO}_3/\text{BaTiO}_3/\text{SrRuO}_3$ capacitors with a $10 \times 10 \mu\text{m}^2$ area displayed an intriguing time-dependent polarization

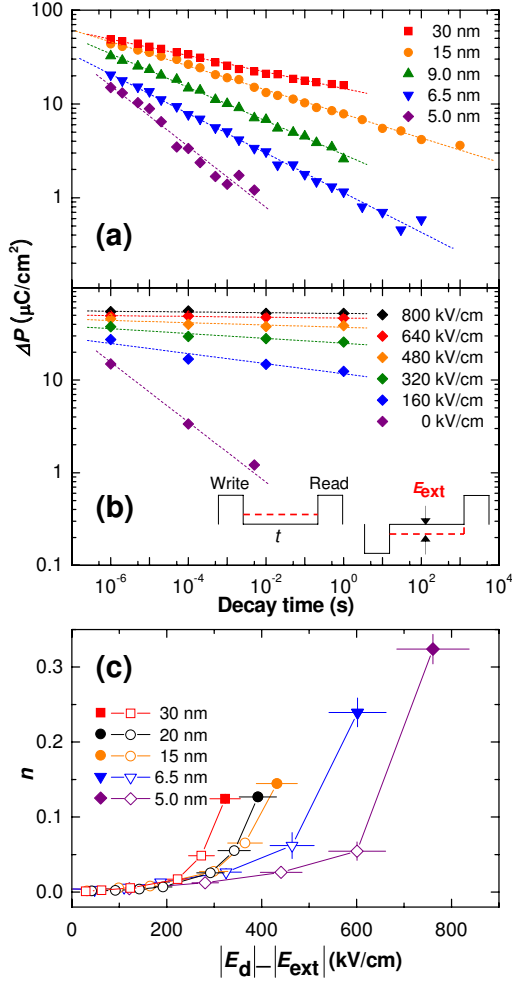


FIG. 2: (color online). (a) Time-dependent net polarization changes, $\Delta P(t)$, without any external field (E_{ext}). (b) $\Delta P(t)$ of the 5.0 nm thick BaTiO₃ capacitor under numerous values of E_{ext} . The left- and right-hand diagrams of the inset show electric pulse trains used to measure non-switching and switching polarizations, respectively. $\Delta P(t)$ corresponds to the difference between these polarizations. (c) The relation between n and the total internal electric field (namely, $|E_d| - |E_{ext}|$). The open and solid symbols correspond to the data with and without E_{ext} , respectively.

decay behavior. We measured the time-dependence of polarization decay using electric write/read pulses separated by a given decay time (t) [9, 15]: the right and the left schematics in the inset of Fig. 2(b) show the electric pulses used to measure the switching and non-switching polarizations, respectively. Figure 2(a) shows that the polarization decay follows a power-law behavior at room temperature [15]: namely, $\Delta P(t) \sim t^{-n}$. As the film becomes thinner, the value of n increases substantially. In particular, for the 5.0 nm thick capacitor, ΔP decays below 1% of its initial value within 10^{-3} s. This rapid polarization decay must be caused by domain backswitching upon removal of the electric field and is

the subject of the discussions that follow.

Within the capacitor geometry, the discontinuity of polarization at the FE/electrode interfaces induces polarization charges. The free carriers inside the electrodes compensate the resulting charge deficit. However, the finite value of the Thomas-Fermi screening length for the free carriers makes the compensation incomplete, resulting in E_d inside the FE layer [17]. It should be noted that the generation of E_d is inevitable, which will limit the performance of most FE capacitor-type devices.

To obtain further information on the detailed effects of E_d on the polarization decay, we measured the time-dependence of ΔP with an external static field E_{ext} , applied in the opposite direction to that of E_d during the electric pulse measurements, displayed schematically by the red dashed lines in the inset of Fig. 2(b) [15]. Since E_{ext} will partially cancel out E_d , it will slow down the polarization decay and consequently reduce the values of n . As shown in Fig. 2(b), n decreases significantly with an increase of E_{ext} and should finally become zero when E_{ext} becomes nearly the same as E_d . This E_{ext} value at $n \sim 0$ provides an experimental value for E_d [15]. For the 5.0 nm thick BaTiO₃ film, E_d can be as large as 800 kV/cm. Note that this value of E_d is even larger than the coercive field value, *i.e.* about 300 kV/cm, which was measured from direct P - E hysteresis measurements [1].

Figure 2(c) shows the dependence of n on the total internal electric field, *i.e.* $|E_d| - |E_{ext}|$, for the BaTiO₃ capacitors. The abscissa-values of the solid symbols, which were measured with $E_{ext} = 0$, correspond to the experimentally estimated E_d values. They clearly show that E_d becomes larger as d_{BTO} becomes smaller. As the $|E_d| - |E_{ext}|$ increases, the values of n increases for all samples. However, we could not find any simple universal relation between n and $|E_d| - |E_{ext}|$.

Further insights could be obtained by looking into the mechanism of domain switching dynamics in an ultrathin FE film. Note that decrease of ΔP means an increase in the number of FE domains with a reversed polarization. It is generally believed that the growth of the opposite domains occurs in three processes, namely (a) formation of nuclei with opposite polarization, (b) their forward growth, and (c) sidewise growth (called, the domain wall motion). For epitaxial FE films thicker than 100 nm, the domain wall motion has been reported to be very important [10]. However, for ultrathin FE films, domain wall motion becomes extremely slow: for example, the speed of the domain wall motion was estimated to be about 1 nm/s for a 29 nm thick Pb(Zr,Ti)O₃ film [8]. In addition, the forward growth of the nuclei is known to occur very fast (*i.e.* a speed of 1000 m/s) [9], so the very slow domain wall motion could not play a major role in the polarization decay behavior observed in Fig. 2(a). Therefore, we propose that, in the ultrathin FE films, the rapid polarization decay should be caused by nucleation-governed domain dynamics and that the large E_d value could make

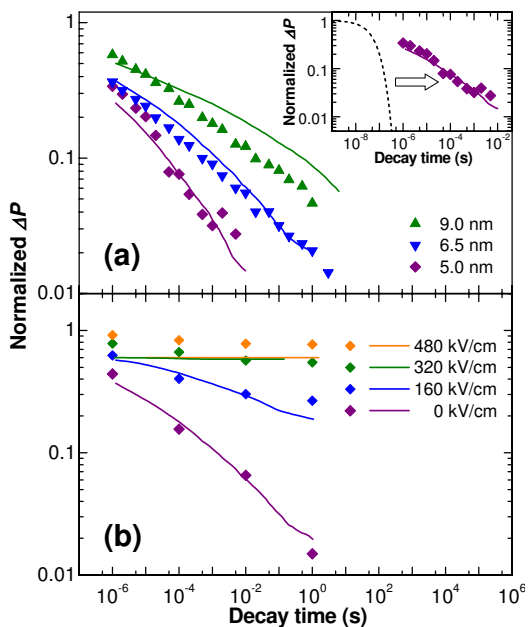


FIG. 3: (color online). (a) Normalized ΔP from the experimental data (the solid symbols) and the Monte-Carlo simulation (the solid lines). The black dotted line in the inset shows the Monte-Carlo simulation results for the 5.0 nm thick BaTiO₃ capacitor without lateral screening of the interaction term between long-range domains in the Hamiltonian. (b) Normalized ΔP of the 5.0 nm thick BaTiO₃ capacitor under numerous values of E_{ext} . The solid symbols and lines correspond to the experimental data and the Monte-Carlo simulation results, respectively.

the thermodynamic nucleation process possible.

Figures 1(b) and 1(c) schematically display formation of nuclei with half-prolate spheroidal and cylindrical shapes, respectively, under an electric field. Here, d is the FE film thickness, and r^* and l^* represent critical radius and length of the half-prolate spheroidal nucleus, respectively. Kay and Dunn calculated the electrostatic energy U for such nuclei formation [18], and showed that there should exist the nucleation energy barrier U^* , as shown in Fig. 1(a). When $l^* < d$, the spheroidal nuclei are likely to be formed, and *vice versa*. They also showed that U^* is proportional to $\sigma_w^3/E^{5/2}$ for the half-prolate nucleus and σ_w^2/E for the cylindrical nucleus [18], where σ_w is the domain wall energy. Using $\sigma_w = 10$ mJ/m² [19], the crossover from the half-prolate spheroidal to cylindrical shapes will occur at $d \sim 10$ nm [20]. Note that the very large E_d values of our ultrathin BaTiO₃ films will make U^* small enough to allow a thermally-activated nucleation process. The experimental E_d values of our BaTiO₃ films are between 300 and 800 kV/cm [15]. With these E_d values, the $U^*/k_B T$ values are estimated to be between 4 and 20 at room temperatures, which are easily accessible by thermal energy.

To explain the observed power-law decay behavior,

we used numerical simulations adopting the Monte-Carlo algorithm, which takes into account the thermally-activated polarization reversal process. We approximated the film to be composed of 128×128 single domain cells lying on the ab -plane, whose size is 2.0 nm and height is the same as the film thickness, with a periodic boundary condition. Each cell has a uniform P , either pointing up or down along the c -axis. We used a dimensionless parameter x ($\equiv P/P_s$), and set the value of x to be either +1 or -1 for the bi-stable states, where P_s is spontaneous polarization. During the switching process, the Hamiltonian H^i per volume V^i of the i -th cell can be expressed as a function of the i -th value of x^i ;

$$H^i = -K_2(x^i)^2 - \frac{\sigma_w d_{BTO}}{2V^i} x^i \sum_{n.n.} r_{n.n.}^i x_{n.n.}^i - E_d^i \cdot P_s x^i - E_{ext} \cdot P_s x^i. \quad (1)$$

The first self-energy term is quite similar to the leading P^2 term in the Landau-Devonshire equation, which provides an approximation of the barrier height between the bi-stable points in the FE potential [21]. The higher order terms P^4 and P^6 were ignored here for the simplicity of the calculations. The second term describes the short-range wall interaction between the nearest neighboring domains, where $r_{n.n.}$ and $x_{n.n.}$ are the adjacent circumference and unit vector of nearest neighbor domain cells, respectively. It has a maximum value when the 4 nearest neighbor domain cells surrounding a nucleated cell have the opposite polarization. The third term originates from the long-range dipolar interaction between cells. The dipolar field E_d^i is the sum of the dipolar electric field caused by all the other cells. The last term describes the work done by external source. A similar calculation method was used in micro-magnetic systems [22].

When two electrodes sandwich a FE film, the electrode screens the value of E_d^i produced by P_s . The screening can occur not only in the perpendicular direction but also in the lateral direction. A numerical estimate reveals that the lateral screening length should be of the order of the FE film thickness. For an ultrathin FE film, only the dipolar interaction between the nearest neighbor domains across domain boundaries could be important, so E_d^i can be approximated to $\hat{e}_d \sum_{n.n.} r_{n.n.}^i x_{n.n.}^i$, where \hat{e}_d is the line density of the dipolar field across the cell boundary. Then, Eq. (1) can be rewritten as

$$H^i = -K_2(x^i)^2 - \frac{\sigma_w^{(eff)} d_{BTO}}{2V^i} x^i \sum_{n.n.} r_{n.n.}^i x_{n.n.}^i - E_{ext} \cdot P_s x^i, \quad (2)$$

where an effective wall energy density $\sigma_w^{(eff)}$ can be defined as $\sigma_w^{(eff)} = \sigma_w + \hat{e}_d P_s 2V^i / d_{BTO}$. Note that the analytic form of the screened dipolar interaction energy

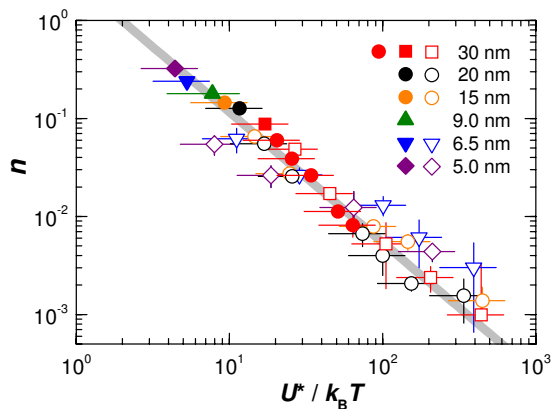


FIG. 4: (color online). A scaling relation between n and $U^*/k_B T$. The open and solid symbols come from the experimental $\Delta P(t)$ data with and without E_{ext} , respectively.

term is identical with that of the domain wall energy. The simulations were performed for room temperature domain dynamics with $K_2 = 3 \times 10^6$ J/m³, $\sigma_w^{(eff)} = -1$ mJ/m², and an attempt frequency of 10^9 Hz.

The Monte-Carlo simulations were performed with and without lateral screening of the interaction term between long-range domains in the Hamiltonian. Without the lateral screening of the interaction term, the simulations for the 5.0 nm thick BaTiO₃ film predicted a very rapid exponential decay of ΔP , as shown by the black dotted line in the inset of Fig. 3(a). When the screened domain interaction term was included as in Eq. (2), the simulations showed that the polarization decay would slow down significantly, exhibiting a power-law behavior, as shown in the inset of Fig. 3(a). The calculated polarization decay agrees with the experimental results quite well. Without changing any other parameter values, we performed the same simulations for other thicknesses of BaTiO₃ capacitors, and found reasonably good agreement, as shown in Fig. 3(a). We also performed similar simulations for the cases with non-zero values of E_{ext} , and obtained good agreement with experimental data, as shown in Fig. 3(b). These results clearly demonstrate that domain dynamics must be governed by thermally-activated nucleation processes in ultrathin films [20].

When the thermodynamic domain nucleation is the governing process for polarization decay, $U^*/k_B T$ should be the most important physical term which determines the decay rate. Following the methods in Ref. [18], we were able to convert the values of $(|E_d| - |E_{ext}|)$ into U^* values and made a plot of n vs. $U^*/k_B T$. Figure 4 demonstrates that there might exist a universal relation between n and $U^*/k_B T$, regardless of d_{BTO} and $(|E_d| - |E_{ext}|)$. To confirm the thermodynamic nucleation-governed polarization switching process, we independently performed polarization decay measurements for the 30 nm thick BaTiO₃ capacitor at various tempera-

tures. The solid red circles in Fig. 4 correspond to the experimental data for temperature-dependent polarization decay, which fall onto the seemingly universal line between n and $U^*/k_B T$. This indicates that there could be a simple relation between n and $U^*/k_B T$, which is universal, irrespective of film thickness, total internal electric field, and temperature.

Our findings about the thermodynamic nucleation-governed switching process and the empirical relation between n and $U^*/k_B T$ have some important implications for the design of nanoscale FE devices. One implication concerns the capacitor geometry of FE devices where the polarization decay due to the E_d is predictable by the empirical relation we found. It could impose a new fundamental thickness limit on such FE devices. For example, ferroelectric random access memories require the retention of a certain value of ΔP for 10 years [9]. For our BaTiO₃ capacitors, U^* should be higher than $40 k_B T$ to retain ΔP at more than 50% of the initial value ($n < 0.02$). This value of U^* corresponds to a thickness of about 40 nm for our fully-strained BaTiO₃ films, which is much thicker than the critical thickness (2.4 nm) for the ferroelectricity of BaTiO₃ [2]. For ultrathin film capacitors, a condition of $U^* \geq A \cdot k_B T$, where A is a constant of the order of 10, has to be satisfied in order to have a stable retention property. As the E_d value increases (decrease in U^*) with the reduction of d_{BTO} , retention loss due to the thermodynamic nucleation of reversed domains becomes much severe. Note that this situation is analogous to that of the superparamagnetic limit for magnetic memory devices: a long-range ferromagnetic order vanishes, when anisotropy energy becomes comparable to thermal fluctuation energy [23].

Our work has clearly shown the importance of a thermodynamic domain nucleation process in the polarization decay of ultrathin FE films. The polarization decay should impose a fundamental thickness limit on capacitor-type devices, which is much stricter than the critical thickness limit. Further experimental and theoretical studies are clearly required to clarify the origin of the empirically-determined relation between n and $U^*/k_B T$ and its applicability to other ultrathin FE systems.

We thank M. W. Kim for discussion. We acknowledge financial support by the Korean Ministry of Education through the BK21 projects and the KOSEF through the CRI Program.

* Electronic address: twnoh@snu.ac.kr

- [1] Y. S. Kim *et al.*, Appl. Phys. Lett. **86**, 102907 (2005).
- [2] J. Junquera and Ph. Ghosez, Nature **422**, 506 (2003).
- [3] D. D. Fong *et al.*, Science **304**, 1650 (2004).
- [4] K. J. Choi *et al.*, Science **306**, 1005 (2004).
- [5] H. N. Lee *et al.*, Nature **433**, 395 (2005).

- [6] I. Kornev, H. Fu, and L. Bellaiche, *Phys. Rev. Lett.* **93**, 196104 (2004).
- [7] Bo-Kuai Lai *et al.*, *Phys. Rev. Lett.* **96**, 137602 (2006).
- [8] T. Tybell, P. Paruch, T. Giamarchi, and J.-M. Triscone, *Phys. Rev. Lett.* **89**, 097601 (2002).
- [9] J. F. Scott, *Ferroelectric Memories* (Springer-Verlag, New York, 2000).
- [10] Y. W. So, D. J. Kim, T. W. Noh, J.-G. Yoon, and T. K. Song, *Appl. Phys. Lett.* **86**, 092905 (2005).
- [11] R. Landauer, *J. Appl. Phys.* **28**, 227 (1957).
- [12] A. Aharoni, *Introduction to the Theory of Ferromagnetism* (Clarendon Press, Oxford, 1996).
- [13] A. M. Bratkovsky and A. P. Levanyuk, *Phys. Rev. Lett.* **85**, 4614 (2000).
- [14] G. Gerra, A. K. Tagantsev, and N. Setter, *Phys. Rev. Lett.* **94**, 107602 (2005).
- [15] D. J. Kim *et al.*, *Phys. Rev. Lett.* **95**, 237602 (2005).
- [16] Y. S. Kim *et al.*, *Appl. Phys. Lett.* **88**, 072909 (2006).
- [17] R. R. Mehta, B. D. Silverman, J. T. Jacobs, *J. Appl. Phys.* **44**, 3379 (1973).
- [18] H. F. Kay and J. W. Dunn, *Phil. Mag.* **7**, 2027 (1962).
- [19] W. J. Merz, *Phys. Rev.* **95**, 690 (1954).
- [20] Our coercive field data agrees well with the prediction for the crossover from the half-prolate spheroidal to cylindrical shapes at $d_{BTO} \sim 10$ nm and also supports the picture of polarization switching dynamics governed by thermodynamic nucleation process in ultrathin ferroelectric films (to be published).
- [21] N. A. Pertsev, A. G. Zembilgotov, and A. K. Tagantsev, *Phys. Rev. Lett.* **80**, 1988 (1998).
- [22] S.-B. Choe and S.-C. Shin, *IEEE Trans. Mag.* **36**, 3167 (2000).
- [23] S. Chikazumi, *Physics of Ferromagnetism* (Oxford Univ. Press, New York, 1997).